European Radiology (2019) 29:5358–5366
https://doi.org/10.1007/s00330-019-06129-4

CHEST

Ultralow-dose CT with knowledge-based iterative model reconstruction (IMR) in evaluation of pulmonary tuberculosis: comparison of radiation dose and image quality

Chenggong Yan[1] · Chunyi Liang[1] · Jun Xu[2] · Yuankui Wu[1] · Wei Xiong[1] · Huan Zheng[1] · Yikai Xu[1]

Received: 7 August 2018 / Revised: 6 February 2019 / Accepted: 6 March 2019 / Published online: 29 March 2019

Abstract

Objectives To evaluate the image quality of ultralow-dose computed tomography (ULDCT) reconstructed with knowledge-based iterative model reconstruction (IMR) in patients with pulmonary tuberculosis (TB).

Methods This IRB-approved prospective study enrolled 59 consecutive patients (mean age, 43.9 ± 16.6 years; F:M 18:41) with known or suspected pulmonary TB. Patients underwent a low-dose CT (LDCT) using automatic tube current modulation followed by an ULDCT using fixed tube current. Raw image data were reconstructed with filtered-back projection (FBP), hybrid iterative reconstruction (iDose), and IMR. Objective measurements including CT attenuation, image noise, and contrast-to-noise ratio (CNR) were assessed and compared using repeated-measures analysis of variance. Overall image quality and visualization of normal and pathological findings were subjectively scored on a five-point scale. Radiation output and subjective scores were compared by the paired Student *t* test and Wilcoxon signed-rank test, respectively.

Results Compared with FBP and iDose, IMR yielded significantly lower noise and higher CNR values at both dose levels ($p < 0.01$). Subjective ratings for pathological findings including centrilobular nodules, consolidation, tree-in-bud, and cavity were significantly better with ULDCT IMR images than those with LDCT iDose images ($p < 0.01$), but blurred edges were observed. With IMR implementation, a 59% reduction of the mean effective dose was achieved with ULDCT (0.28 ± 0.02 mSv) compared with LDCT (0.69 ± 0.15 mSv) without impairing image quality ($p < 0.001$).

Conclusions IMR offers considerable noise reduction and improvement in image quality for patients with pulmonary TB undergoing chest ULDCT at an effective dose of 0.28 mSv.

Key Points

- *Radiation dose is a major concern for tuberculosis patients requiring repeated follow-up CT.*
- *IMR allows substantial radiation dose reduction in chest CT without compromising image quality.*
- *ULDCT reconstructed with IMR allows accurate depiction of CT features of pulmonary tuberculosis.*

Keywords Tomography, X-ray computed · Infection · Thorax · Pulmonary tuberculosis · Radiation dosage

Abbreviations

CNR	Contrast-to-noise ratio
$CTDI_{vol}$	Volume CT dose index
DLP	Dose-length product
DRI	Dose right index
ED	Effective dose
FBP	Filtered-back projection
FOM	Figure of merit
GGO	Ground-glass opacity
IMR	Iterative model reconstruction
IR	Iterative reconstruction
LDCT	Low-dose CT
ROI	Region of interest
TB	Tuberculosis
ULDCT	Ultralow-dose CT

✉ Yikai Xu
yikaixu917@gmail.com

[1] Department of Medical Imaging Center, Nanfang Hospital, Southern Medical University, No. 1838 Guangzhou Avenue North, Guangzhou 510515, Guangdong, People's Republic of China

[2] Department of Hematology, Nanfang Hospital, Southern Medical University, No. 1838 Guangzhou Avenue North, Guangzhou 510515, Guangdong, People's Republic of China

Introduction

Tuberculosis (TB) remains the leading cause of death attributed to an infectious disease worldwide, responsible for an estimated 1.67 million deaths annually [1]. Nonspecific clinical signs and symptoms delay the effective treatment in affected patients and result in onward transmission of TB [2]. Chest radiography is the primary imaging modality used in the assessment of suspected TB. But it can be negative in many patients (up to 15%) with proven TB [3]. CT is more effective than chest radiographs in the detection and management of the chronic disease. For patients with primary diagnosis of pulmonary TB, routine treatment was maintained for at least 6 months, including multiple follow-up CT examinations performed at 2- or 4-month intervals during the course of illness [2]. However, repeated follow-up CTs pose concerns over a high cumulative radiation exposure for patients with TB, especially in pediatric patients and young women. In order to keep the principle "as low as reasonably achievable" (ALARA), a dose-reduced chest CT protocol without compromising the image quality and diagnostic accuracy would be desirable [4].

Different hybrid iterative reconstruction (IR) techniques have recently been introduced to clinical routine, enabling significant noise reduction in reduced dose CT protocols compared with the conventional filtered-back projection (FBP) [5, 6]. The modeling of photon and noise statistics is incorporated into the iDose™ (Philips Healthcare) algorithm, which allows dose reduction by 32–65% without increasing noise in the hybrid IR images [7, 8]. More recently, a more advanced knowledge-based iterative model reconstruction (IMR) is available in clinical practice [9]. The notable feature of IMR is that knowledge of data statistics, image statistics, and system models are taken into account in the optimization process to reduce image noise and improve spatial resolution [10]. However, only a few studies have evaluated the effects of knowledge-based IMR on ultralow-dose CT (ULDCT) in the assessment of pulmonary infectious lesions [11, 12].

Hence, the purpose of this study was to assess lesion depiction and image quality on ULDCT reconstructed with IMR in patients with pulmonary TB.

Materials and methods

This prospective single-institution study was compliant with the Human Insurance Portability and Accountability Act (HIPAA) guidelines and was approved by our institutional review board. All patients provided written informed consent.

Patient population

From March 2017 to June 2018, 59 patients (mean age, 43.9 years; age range, 18–78 years) known or suspected to have primary or secondary TB were prospectively enrolled. Inclusion criteria were as follows: (a) prior cross-sectional imaging examinations for follow-up or abnormal radiography findings for further diagnosis and (b) positive *Mycobacterium tuberculosis* culture from sputum, bronchoalveolar lavage, or lung biopsy sample. The exclusion criteria were pregnancy or patients younger than 18 years.

CT technique

All CT images were acquired with a 256-slice multi-detector row CT scanner (Brilliance iCT; Philips Healthcare). The ULDCT scans were performed immediately after the low-dose CT (LDCT) by using identical scanning parameters, with the exception of dose right index (DRI, and therefore tube current) and tube voltage. Scanning parameters are given in Table 1. Image series were not performed in a single breath-hold with a delay of an average 5 s between the acquisitions.

CT image reconstruction

Raw data were reconstructed with FBP, iDose4 (Level 4), and IMR (Philips Healthcare) techniques using the standard kernel at 1 mm (Fig. 1). As for IMR image reconstruction, Level 1 Sharp plus was selected based on previous literature [12]. Thus, six image data sets (two radiation dose settings and three reconstruction algorithms) were generated in each patient. All 354 datasets were used for objective image analysis. For subjective assessment, the ULDCT IMR images were compared with the LDCT iDose images in all 59 patients.

Table 1 CT image acquisition parameters

	LDCT	ULDCT
Peak tube voltage (kVp)	100	80
Tube current modulation	Automatic exposure control	Fixed tube current
Tube current-time product (mAs)	DRI = 4	25
Pitch	0.985	0.985
Collimation (mm)	128 × 0.625	128 × 0.625

LDCT, low-dose CT; *ULDCT*, ultralow-dose CT; *DRI*, dose right index

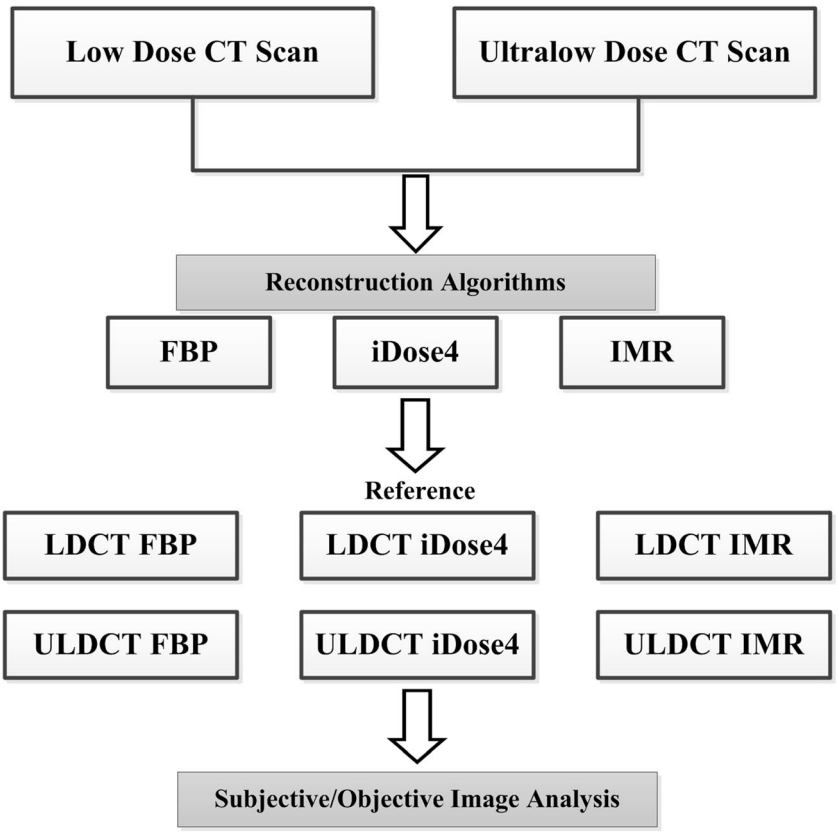

Fig. 1 Flowchart shows CT image acquisitions at low-dose and ultralow-dose CT with three different reconstruction algorithms (filtered-back projection, FBP; hybrid iterative reconstruction, iDose; iterative model reconstruction, IMR)

All images were anonymized, and the data sets were coded and randomized before blinded evaluation.

Objective image analysis

For image noise and the contrast-to-noise ratio (CNRs) analysis in the chest, circular regions of interest (ROIs) were manually placed within the aortic arch and the homogeneous area of the normal lung parenchyma at the level of the carina. Noise was defined as the standard deviations of the ROIs that occupied at least two-thirds of the aortic lumen and not including the wall of the aorta. Calcifications, large vessels and bronchi, and areas with prominent streak artifacts were carefully avoided. For all measurements, the size, shape, and location of the ROIs were kept constant among different image series by applying a copy and paste function at the workstation. CNRs relative to the aorta for the lung parenchyma were calculated using the following equation: $CNR = |ROI_l - ROI_a|/N$, where ROI_l is the mean attenuation for the bilateral lung parenchyma, ROI_a is the mean attenuation for the aorta, and N is the mean image noise. The noise was normalized to effective dose (ED) by using a figure of merit (FOM) for the noise (FOM_N), which was defined as follows:

$$FOM_N = 1/N^2 \times ED.$$

Table 2 Objective image quality according to reconstruction algorithms and radiation dose

		LDCT			ULDCT		*p* value*
	FBP	iDose	IMR	FBP	iDose	IMR	
CT value (HU)	45.82 ± 8.83	45.74 ± 8.23	45.36 ± 7.33	46.70 ± 6.96	45.78 ± 7.16	45.79 ± 7.48	0.964
Noise (HU)	52.15 ± 10.45	34.77 ± 6.05	15.61 ± 1.81	79.30 ± 22.57	47.80 ± 9.64	18.16 ± 1.95	< 0.001
CNR	18.50 ± 3.73	27.37 ± 5.14	60.32 ± 7.84	13.78 ± 9.95	19.87 ± 4.26	51.59 ± 5.86	< 0.001
FOM_N ($\times 10^{-4}$)	6.45 ± 3.52	14.13 ± 7.37	66.09 ± 26.05	7.00 ± 3.93	17.34 ± 6.54	111.56 ± 24.89	< 0.001

Data are mean values with standard deviation

LDCT, low-dose CT; *ULDCT*, ultralow-dose CT; *FBP*, filtered-back projection; *IMR*, iterative model reconstruction; *HU*, Hounsfield unit; *CNR*, contrast-to-noise ratio; *FOMN*, figure of merit for the noise

*Repeated-measures analysis of variance

Table 3 Comparison of subjective grading for image quality and visibility of normal and pathological findings between ULDCT IMR and LDCT iDose

	ULDCT IMR	LDCT iDose	*p* value*
Overall image quality (5/4/3/2/1)	0/27/31/1/0	0/0/18/41/0	0.000
Normal structures (5/4/3/2/1)			
Large bronchi	35/23/1/0/0	4/43/12/0/0	0.000
Peripheral vessels	12/27/20/0/0	1/41/17/0/0	0.150
Fissures	0/8/34/17/0	0/25/34/0/0	0.000
Pathological findings (5/4/3/2/1)			
Centrilobular nodule ($n = 48$)	26/21/1/0/0	3/31/4/0/0	0.000
Fibrosis ($n = 44$)	14/25/5/0/0	2/23/18/1/0	0.000
Calcification ($n = 42$)	41/1/0/0/0	39/3/0/0/0	0.317
Consolidation ($n = 35$)	14/20/1/0/0	0/17/18/0/0	0.000
Tree-in-bud ($n = 20$)	4/11/4/1/0	0/9/11/0/0	0.020
Cavity ($n = 16$)	11/5/0/0/0	1/10/5/0/0	0.001
Lymphadenopathy ($n = 13$)	8/5/0/0/0	0/9/4/0/0	0.003
GGO ($n = 9$)	0/8/1/0/0	0/4/5/0/0	0.102

Subjective five-point grading scale (a score of 5 represented the best rating and a score of 1 the worst rating)
ULDCT, ultralow-dose CT; *IMR*, iterative model reconstruction; *LDCT*, low-dose CT; *GGO*, ground-glass opacity
*Wilcoxon signed-rank test

Subjective image analysis

Two radiologists who were blinded to the technical scanning parameters independently evaluated the image sets on a post-processing workstation. The overall image quality was rated on a five-point scale (1 = unacceptable image for diagnostic purposes, 2 = somewhat suboptimal image with above average noise, 3 = an acceptable image with average noise, 4 = satisfactory image with less than average noise, and 5 = excellent overall image with minimum noise) [13]. Normal lung structures were evaluated according to three categories: proximal bronchi and vessels, peripheral bronchi/bronchioles and vessels, and fissures. Similarly, the presence of pathological findings including centrilobular nodules, lobar/subsegmental consolidations, tree-in-bud (centrilobular small nodules and branching

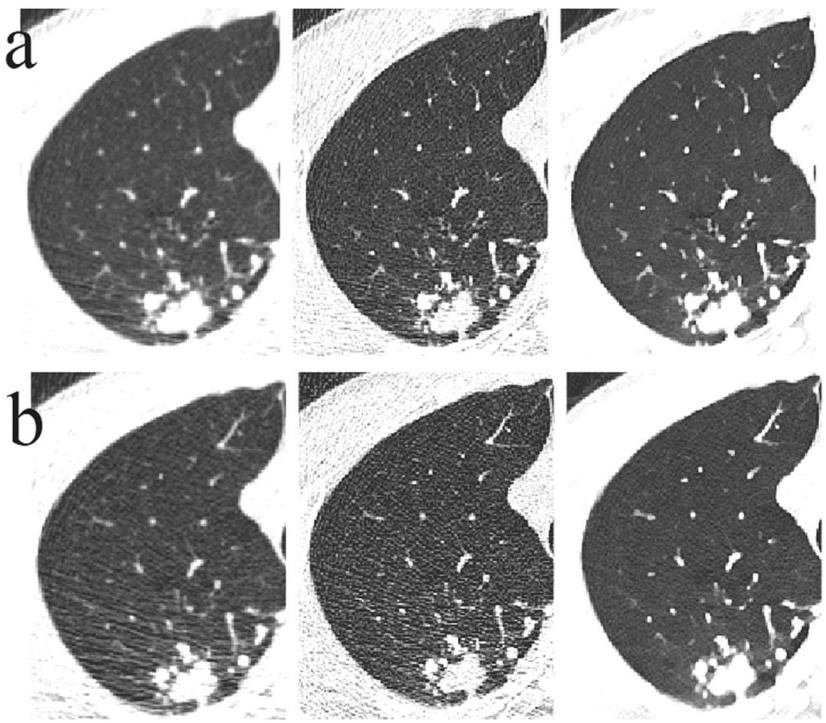

Fig. 2 Chest CT images obtained in a 36-year-old man (BMI, 20.86 kg/m^2) with infiltrative TB show a pulmonary nodule with surrounding satellite lesions in the right upper lobe. These findings can be detected with LDCT ($CTDI_{vol}$, 1.3 mGy; **a**) and ULDCT ($CTDI_{vol}$, 0.5 mGy; **b**) reconstructed with FBP, iDose, and IMR

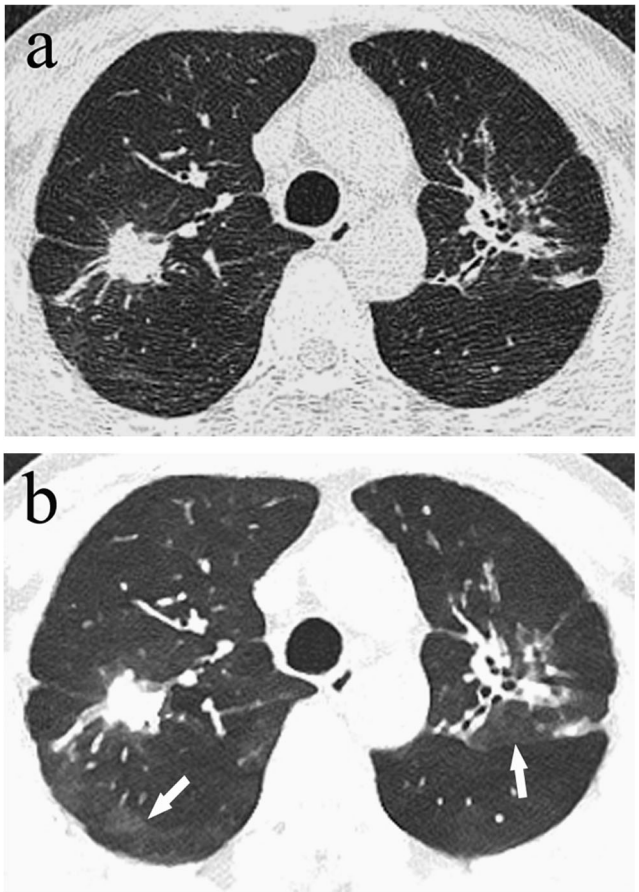

Fig. 3 Chest CT axial images obtained in a 51-year-old man (BMI, 21.30 kg/m^2) with TB are shown in the lung window. A nodule in the right upper lobe, centrilobular micronodules in the left upper lobe and fibrosis in bilateral upper lobes are clearly visualized on both LDCT iDose (**a**, $CTDI_{vol}$, 1.1 mGy) and ULDCT IMR (**b**, $CTDI_{vol}$, 0.4 mGy). Note the blotchy, pixellated appearance (arrows) in **b** compared with **a**

structures), thick wall cavitation, ground-glass opacity (GGO), calcification, fibrosis, and lymphadenopathy was assessed. Then, both reviewers independently scored the normal and pathological pulmonary findings as follows [12]: 5 = excellent visibility of structures with no blurring; 4 = good visibility of structures with slight blurring; 3 = satisfactory visibility of structures with moderate blurring, but enough for diagnosis; 2 = poor visibility of structures with major blurring and could not be used for diagnosis; and 1 = very hard to distinguish the fine structures.

Assessment of radiation dose

The volume CT dose index ($CTDI_{vol}$) and dose-length product (DLP) were recorded from the scanner dose report. Estimated ED was calculated from the total DLP by using a constant of 0.014 mSv/(mGy × cm).

Statistical analyses

All statistical analyses were performed using SPSS software (version 21.0, SPSS Inc.). Mean image noise, CNR, and the corresponding FOM_N were compared among different image series using repeated-measures analysis of variance with Dunnett's post testing for multiple comparisons. Differences in the radiation dose parameters between the two scanning protocols were determined with paired Student t tests. Subjective scores were compared by the Wilcoxon signed-rank test. A p value of less than .05 was considered to indicate a significant difference.

Results

Objective image analysis

The results of the CT values, noise, CNR, and FOM_N according to the CT acquisitions and reconstruction techniques are shown in Table 2. The mean CT values within the aorta did not differ significantly ($p > 0.10$) across all reconstruction algorithms and scanning protocols. The reduction in image noise and the increase in CNR according to reconstruction algorithms were significant on IMR-reconstructed images compared with iDose or FBP images at both radiation dose settings (Dunnett's post test, $p < 0.001$). An increase in radiation dose was significantly associated with decreased noise and increased CNR, whatever reconstruction algorithms (all $p < 0.001$). However, when noise was normalized to effective dose, our FOM_N results indicated that the use of ULDCT IMR led to a nearly 87% decrease in noise compared with the noise at LDCT iDose ($p < 0.001$).

Subjective image analysis

The subjective scores for overall image quality and visibility of normal and pathological findings are displayed in Table 3. Overall image quality for ULDCT IMR was rated as significantly better than that of LDCT iDose ($p < 0.05$). The visualization of all normal pulmonary structures except for fissures on LDCT iDose images was substantially non-inferior on ULDCT reconstructed with IMR images.

The most common radiological patterns for pulmonary TB were centrilobular nodules (48/59, 81.4%), fibrosis (74.6%), and calcification (71.2%), followed by lobar/subsegmental consolidation (59.3%), tree-in-bud (33.9%), thick wall cavitation (27.1%), lymphadenopathy (22.0%), and GGO (15.3%). In the qualitative assessment of pathological pulmonary findings, no remarkable differences were observed in the distribution of subjective scores for calcification and GGO between the two groups ($p > 0.05$). In addition, other typical findings of TB on ULDCT IMR images (Figs. 2, 3, 4, and 5) were rated as significantly better than those on LDCT iDose (all $p < 0.05$), but blurred edges were observed.

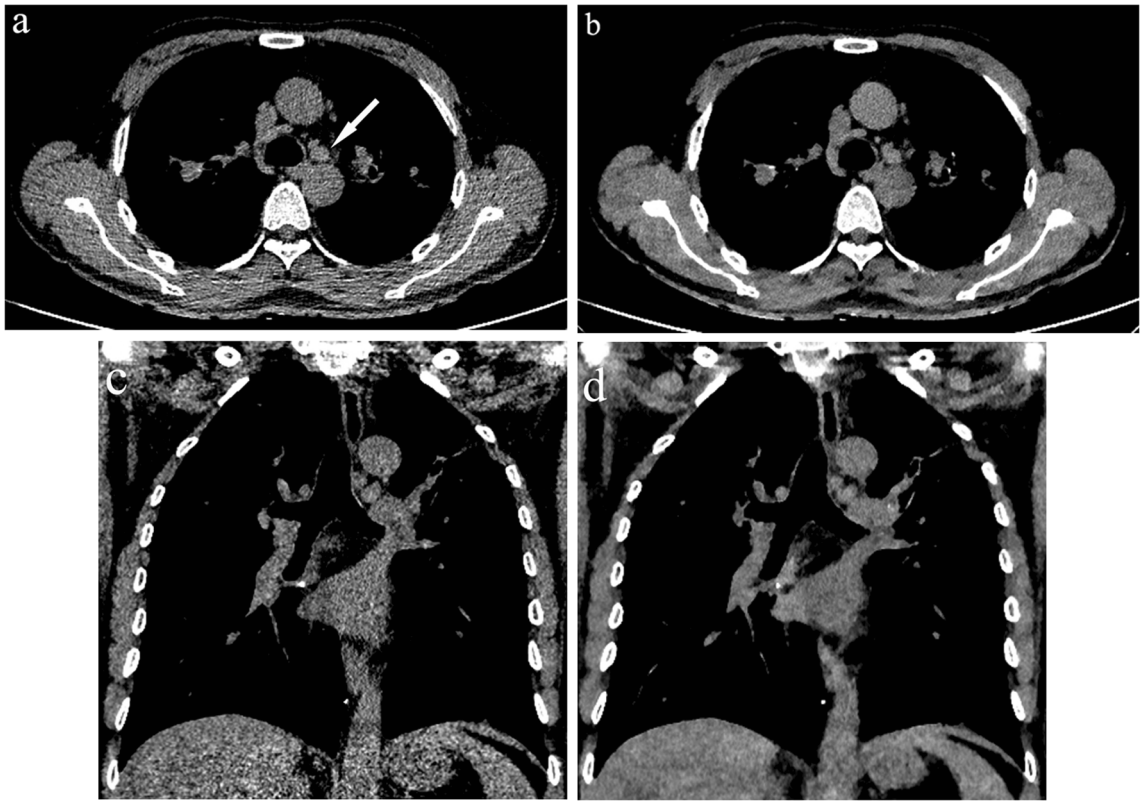

Fig. 4 Chest CT axial (**a**, **b**) and coronal (**c**, **d**) images obtained in a 53-year-old man (BMI, 20.66 kg/m^2) with TB are shown in the mediastinal window. Multiple enlarged lymph nodes in mediastinum (arrow) are clearly visualized on both LDCT iDose (**a, c**; $CTDI_{vol}$, 1.2 mGy) and ULDCT IMR (**b, d**; $CTDI_{vol}$, 0.5 mGy)

Effective dose

Average radiation doses are summarized in Table 4. On average, the reduction in mean radiation output based on size-specific dose estimate was 59% (0.28/0.69 mSv) for ULDCT protocol compared with that of the LDCT protocol.

Discussion

In this study, we assessed the feasibility of ULDCT ($CTDI_{vol}$, 0.49 mGy) acquired with low-tube-voltage and low-tube-current for the detection of pulmonary TB by using the latest generation of knowledge-based IMR. Our study results demonstrate that the described IMR algorithm enables a significant reduction of radiation dose without compromising image quality in patients with pulmonary TB.

CT is generally regarded as the gold standard for assessing the lung abnormalities including TB [14]. It also effectively helps to distinguish between active and inactive TB [15]. With the increasing use of CT, concerns of radiation-induced carcinogenesis are important. Therefore, high accumulative radiation doses from multiple follow-up CT examinations are criticized, especially in young patients with proven diagnosis of pulmonary TB. Lung MRI has emerged as a harmless imaging alternative to CT for depicting infectious lesions [16]. However, lesions less than 5 mm may be missed and are thus limited by the low lesion contrast on partial volume effects. Recent studies indicate that radiation exposure for spiral CT can be optimized by reduced dose scans reconstructed by novel fully IR algorithm while maintaining lesion depiction [17].

Several prior clinical studies clearly demonstrated that CT images reconstructed with various types of IR allow for substantial dose reduction while maintaining diagnostic acceptability compared with FBP images [5, 6]. IMR is one of the most recently introduced model-based IR algorithms, which uses a noise modeling technique to accurately determine the data and image statistics and the system models. Zhang et al [18] reported a dose reduction by approximately 44% for chest ULDCT (0.67 ± 0.08 mSv) reconstructed with IMR without significant loss of image quality for lung screening compared with LDCT protocol (1.20 ± 0.08 mSv). Our results indicate that a radiation dose level of 0.28 mSv for lung CT is feasible, which is reduced by nearly 90.67% compared with the standard dose level reported by Pourjabbar et al [19]. For better visualization of lymph nodes in the mediastinal windows, we did not decrease the radiation dose output to the level of

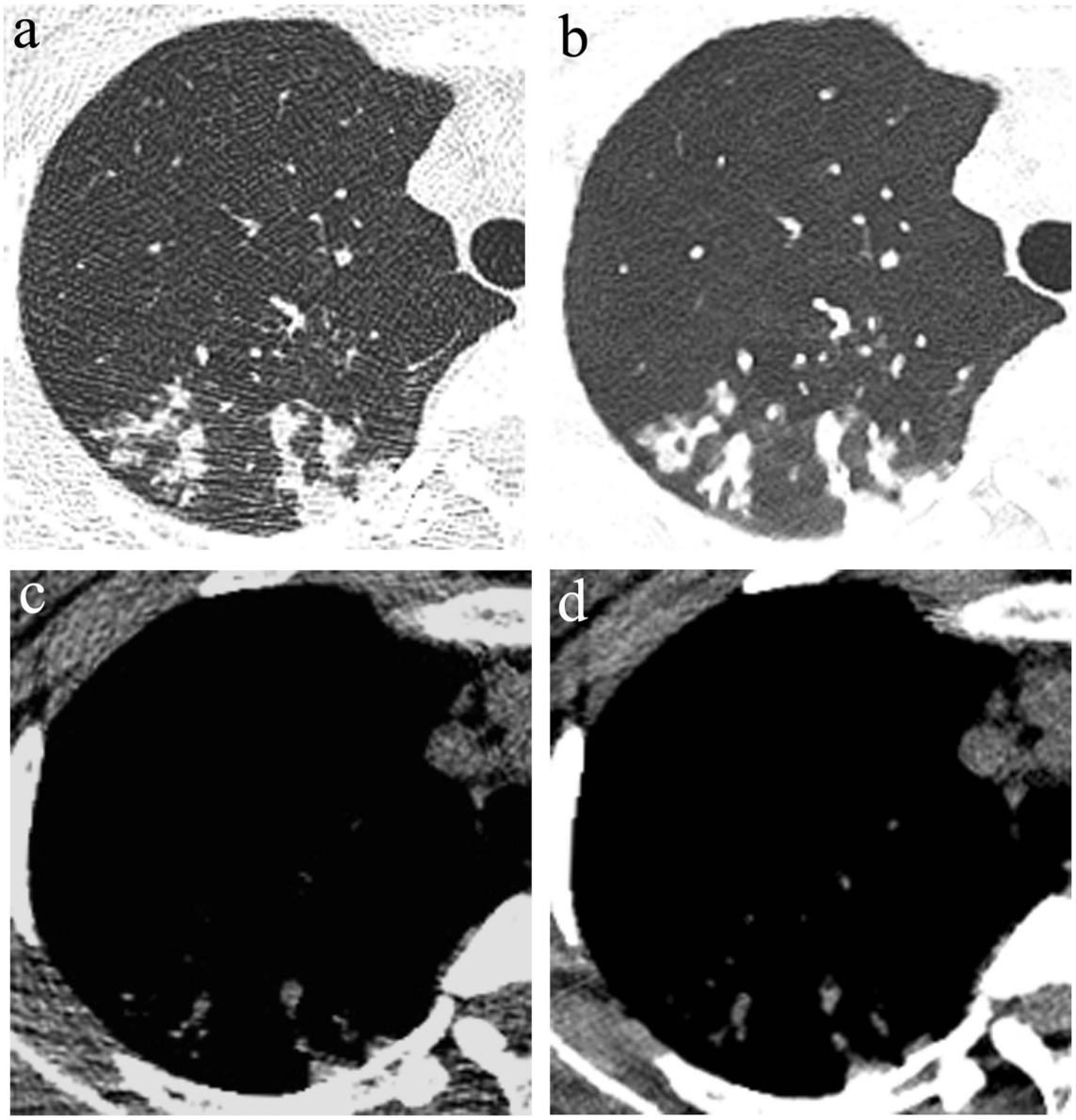

Fig. 5 Transverse LDCT ($CTDI_{vol}$, 1.0 mGy) reconstructed with iDose image (**a**, **c**) of a 27-year-old woman (BMI, 20.96 kg/m^2) with suspected TB shows a patchy consolidation with surrounding tree-in-bud sign in the right upper lobe. Both findings are also detected on ULDCT ($CTDI_{vol}$, 0.4 mGy) with IMR (**b**, **d**), but slight blurring can be observed

0.2 mSv. Likewise, Hata et al [20] have recently reported that model-based iterative reconstruction (MBIR, GE Healthcare) enables dose reduction down to 0.18 ± 0.02 mSv for pulmonary emphysema quantification. However, the computational time of reportedly 50 min per single chest CT image series for MBIR severely limits its routine use in clinical practice [21]. In comparison, IMR provides reasonably fast reconstruction speed of less than 5 min for routine chest CT.

Table 4 Data for radiation dose

	CTDIvol (mGy)	DLP (mGy cm)	Effective dose (mSv)
LDCT	1.21 ± 0.27	49.13 ± 10.86	0.69 ± 0.15
ULDCT	0.49 ± 0.02	20.18 ± 1.69	0.28 ± 0.02

Data are mean values with standard deviation

LDCT, low-dose CT; *ULDCT*, ultralow-dose CT; *$CTDI_{vol}$*, volume CT dose index; *DLP*, dose-length product

The qualitative image assessment showed significantly higher scores for the image quality in ULDCT reconstructed with IMR compared with LDCT iDose, similar to other published reports [11, 22]. The benefit of dose reduction is most likely relevant to those patients requiring sequential follow-up studies for pulmonary TB. Interestingly, we noted that although ULDCT IMR images had significantly

lower objective image noise compared with LDCT iDose, a blotchy pixelated image appearance was noted on IMR images. Our results are consistent with previous studies using different hybrid and fully IR techniques at higher settings [23–25]. Despite having better image quality than hybrid IR iDose4, ULDCT IMR images were suboptimal for the evaluation of conspicuity of the interlobar fissures, which may be responsible for aggressive denoising of images or lack of edge enhancement [26]. However, visibility of large bronchi and peripheral vessels was not impaired in ULDCT IMR images, most likely owing to the high inherent contrast of these structures [27]. In addition, the visibility of pathologic findings was rated as unimpaired on ULDCT IMR images for the depiction of typical imaging features suggestive of TB including centrilobular nodules, consolidation, tree-in-bud, and cavity.

This study has several limitations. First, the sample size was relatively small because of the ethical considerations associated with additional radiation exposure from research CT acquisition. Second, we have assessed only two radiation dose settings and only iterative reconstruction methods from a single vendor. The iDose4 level for ULDCT and LDCT was subjectively selected according to the settings routinely used in our department. Third, owing to the differences in inherent appearance among IMR, iDose4 and FBP images, it was difficult to truly blind the radiologists during subjective image analysis.

In conclusion, ULDCT at 80 kVp and 25 mAs with an effective dose of 0.28 mSv generates images of diagnostic quality in patients with pulmonary TB with the assistance of knowledge-based IMR reconstruction.

Acknowledgements The authors would like to thank Dr. Yan Jiang from the Philips Healthcare for providing technical support.

Funding This study has received funding by the National Key Research and Development Program of China (grant 2016YFC0107104) and the Science and Technology Planning Project of Guangdong Province, China (grant 2015B010131011).

Compliance with ethical standards

Guarantor The scientific guarantor of this publication is Prof. Yikai Xu.

Conflict of interest The authors of this manuscript declare no relationships with any companies, whose products or services may be related to the subject matter of the article.

Statistics and biometry No complex statistical methods were necessary for this paper.

Informed consent Written informed consent was obtained from all subjects (patients) in this study.

Ethical approval Institutional Review Board approval was obtained.

Methodology
- prospective
- observational
- performed at one institution

References

1. Zumla A, George A, Sharma V et al (2015) The WHO 2014 global tuberculosis report–further to go. Lancet Glob Health 1:e10–e12
2. Atun R, Weil DE, Eang MT, Mwakyusa D (2010) Health-system strengthening and tuberculosis control. Lancet 9732:2169–2178
3. Wormanns D (2012) Radiological imaging of pulmonary tuberculosis. Radiologe 2:173–184
4. Hara AK, Wellnitz CV, Paden RG, Pavlicek W, Sahani DV (2013) Reducing body CT radiation dose: beyond just changing the numbers. AJR Am J Roentgenol 1:33–40
5. Berlin SC, Weinert DM, Vasavada PS et al (2015) Successful dose reduction using reduced tube voltage with hybrid iterative reconstruction in pediatric abdominal CT. AJR Am J Roentgenol 2:392–399
6. Laqmani A, Veldhoen S, Dulz S et al (2016) Reduced-dose abdominopelvic CT using hybrid iterative reconstruction in suspected left-sided colonic diverticulitis. Eur Radiol 1:216–224
7. Khawaja RD, Singh S, Blake M et al (2015) Ultralow-dose abdominal computed tomography: comparison of 2 iterative reconstruction techniques in a prospective clinical study. J Comput Assist Tomogr 4:489–498
8. Den Harder AM, Willemink MJ, van Hamersvelt RW et al (2016) Effect of radiation dose reduction and iterative reconstruction on computer-aided detection of pulmonary nodules: intra-individual comparison. Eur J Radiol 2:346–351
9. Iyama Y, Nakaura T, Iyama A et al (2017) Feasibility of iterative model reconstruction for unenhanced lumbar CT. Radiology 1:153–160
10. Sauter A, Koehler T, Brendel B et al (2018) CT pulmonary angiography: dose reduction via a next generation iterative reconstruction algorithm. Acta Radiol. https://doi.org/10.1177/0284185118784976
11. Yan C, Xu J, Liang C et al (2018) Radiation dose reduction by using CT with iterative model reconstruction in patients with pulmonary invasive fungal infection. Radiology 1:285–292
12. Laqmani A, Avanesov M, Butscheidt S et al (2016) Comparison of image quality and visibility of normal and abnormal findings at submillisievert chest CT using filtered back projection, iterative model reconstruction (IMR) and iDose(4). Eur J Radiol 11:1971–1979
13. Pontana F, Billard AS, Duhamel A et al (2016) Effect of iterative reconstruction on the detection of systemic sclerosis-related interstitial lung disease: clinical experience in 55 patients. Radiology 1:297–305
14. Skoura E, Zumla A, Bomanji J (2015) Imaging in tuberculosis. Int J Infect Dis 32:87–93
15. Yeh JJ, Yu JK, Teng WB et al (2012) High-resolution CT for identify patients with smear-positive, active pulmonary tuberculosis. Eur J Radiol 1:195–201
16. Yan C, Tan X, Wei Q et al (2015) Lung MRI of invasive fungal infection at 3 Tesla: evaluation of five different pulse sequences and comparison with multidetector computed tomography (MDCT). Eur Radiol 2:550–557
17. Mileto A, Zamora DA, Alessio AM et al (2018) CT detectability of small low-contrast hypoattenuating focal lesions: iterative reconstructions versus filtered back projection. Radiology 2:443–454

18. Zhang M, Qi W, Sun Y, Jiang Y, Liu X, Hong N (2017) Screening for lung cancer using sub-millisievert chest CT with iterative reconstruction algorithm: image quality and nodule detectability. Br J Radiol 1090:20170658
19. Pourjabbar S, Singh S, Kulkarni N et al (2015) Dose reduction for chest CT: comparison of two iterative reconstruction techniques. Acta Radiol 6:688–695
20. Hata A, Yanagawa M, Kikuchi N, Honda O, Tomiyama N (2018) Pulmonary emphysema quantification on ultra-low-dose computed tomography using model-based iterative reconstruction with or without lung setting. J Comput Assist Tomogr 5:760–766
21. Neroladaki A, Botsikas D, Boudabbous S, Becker CD, Montet X (2013) Computed tomography of the chest with model-based iterative reconstruction using a radiation exposure similar to chest X-ray examination: preliminary observations. Eur Radiol 2:360–366
22. Park HJ, Lee JM, Park SB, Lee JB, Jeong YK, Yoon JH (2016) Comparison of knowledge-based iterative model reconstruction and hybrid reconstruction techniques for liver CT evaluation of hypervascular hepatocellular carcinoma. J Comput Assist Tomogr 6:863–871
23. Padole A, Singh S, Ackman JB et al (2014) Submillisievert chest CT with filtered back projection and iterative reconstruction techniques. AJR Am J Roentgenol 4:772–781
24. Lee SW, Kim Y, Shim SS et al (2014) Image quality assessment of ultra low-dose chest CT using sinogram-affirmed iterative reconstruction. Eur Radiol 4:817–826
25. Vardhanabhuti V, Pang CL, Tenant S, Taylor J, Hyde C, Roobottom C (2017) Prospective intra-individual comparison of standard dose versus reduced-dose thoracic CT using hybrid and pure iterative reconstruction in a follow-up cohort of pulmonary nodules-effect of detectability of pulmonary nodules with lowering dose based on nodule size, type and body mass index. Eur J Radiol 91:130–141
26. de Margerie-Mellon C, de Bazelaire C, Montlahuc C et al (2016) Reducing radiation dose at chest CT: comparison among model-based type iterative reconstruction, hybrid iterative reconstruction, and filtered Back projection. Acad Radiol 10:1246–1254
27. Khawaja RD, Singh S, Gilman M et al (2014) Computed tomography (CT) of the chest at less than 1 mSv: an ongoing prospective clinical trial of chest CT at submillisievert radiation doses with iterative model image reconstruction and iDose4 technique. J Comput Assist Tomogr 4:613–619